

## FLOOD SUSCEPTIBILITY ASSESSMENT IN THE NERA RIVER BASIN USING GIS: IMPACTS ON LAND USE AND LAND COVER

Loredana COPĂCEAN<sup>1</sup>, Luminița COJOCARIU<sup>1,2</sup>

<sup>1</sup>University of Life Sciences “King Mihai I” from Timișoara,  
119 Calea Aradului Street, 300645, Timișoara, Romania

<sup>2</sup>Agricultural Research and Development Station Lovrin,  
200 Principala Street, 307250, Lovrin, Romania

Corresponding author email: luminita\_cojocariu@usvt.ro

### Abstract

*Floods, rapid and destructive phenomena, significantly impact the environment, including agricultural lands. Geospatial methods for analysis, mapping, and monitoring have been developed over time to identify vulnerable areas. In this context, the present study applies a complex GIS model based on geospatial data, remote sensing data and the Analytic Hierarchy Process (AHP) to determine flood susceptibility in the Nera river basin, located in the southwest of Romania (Carăș-Severin County). The analysis includes nine factors: precipitation, drainage density, elevation, slope, distance to rivers, soils, topography, land use and land cover (LULC) and distance to roads. The results are synthesized into a susceptibility map, classified by risk levels and correlated with LULC to evaluate the impact on agriculture. Theoretically and practically, such models are essential for preventing and managing the effects of floods and for implementing optimal measures in line with sustainable development principles*

**Key words:** GIS models, flood susceptibility, watershed, impact, agricultural land.

### INTRODUCTION

Floods, destructive events with rapid occurrence, are among the most damaging hydro-geomorphological phenomena (Khosh et al., 2022). They result from the complex interaction of natural and anthropogenic factors, affecting the hydrological regime of river basins in various ways and proportions (Papaioannou et al., 2018; Syarifudin et al., 2022). These phenomena have significant effects on both the environment and society, causing loss of human lives, infrastructure damage, and public health issues, including the contamination of drinking water sources (Peker et al., 2024).

The impact of floods on agricultural land manifests through complex abiotic stress, affecting light availability, soil oxygenation, and nutrient cycling (Wang et al., 2022; Barneze et al., 2023). These changes alter soil properties and reduce fertility (Arabameri et al., 2020), negatively impacting plant growth and crop productivity (Bharadwaj et al., 2023).

To better understand and manage the impact of floods on agricultural land, the use of advanced hydrological risk modeling methods is essential. These methods have continuously evolved,

enabling more precise identification of flood-prone areas.

Being dynamic and complex phenomena (Swain et al., 2020), floods are most effectively analyzed and mapped using geomatic techniques (Cai et al., 2021; Hagos et al., 2022; Covaci et al., 2023; Copăcean et al., 2025). Methods used for susceptibility assessment include Multi-Criteria Decision Analysis (MCDA) (Souissi et al., 2019) and the Analytic Hierarchy Process (AHP) (Chen et al., 2015), applied globally, including in river basins in Romania (Costache & Zaharia, 2017; Dragomir et al., 2020; Popescu & Bărbulescu, 2023). These methods contribute to identifying vulnerable areas and implementing measures to mitigate the effects on soil and agricultural crops.

In this context, the present study applies a complex spatial analysis model in a GIS environment, based on Multi-Criteria Decision Analysis (MCDA) and the Analytic Hierarchy Process (AHP), to identify flood-prone areas in the Nera River basin and assess their potential impact on agricultural land.

The main objectives include: (1) analyzing the physical-geographical conditions; (2) selecting

and evaluating relevant factors in flood occurrence; (3) creating thematic maps of the involved factors; (4) classifying the basin territory according to flood susceptibility, and (5) analyzing the impact of floods on agricultural land.

## MATERIALS AND METHODS

### Study area

The Nera River basin, covering 138,084 hectares, is located in southwestern Romania along the Serbian border (Figure 1). It is bordered by the hydrographic basins of the Caraș, Cerna, and Danube rivers. The hydrographic network is well-defined, with the

Nera river having numerous tributaries, whose sources are in the adjacent mountainous area. The relief varies considerably, with altitudes ranging between 62 m and 1430 m (Figure 1), an aspect that is reflected in the geographical and hydrographic characteristics of the region (Simon et al., 2022) and, further, in hydrogeomorphological phenomena, water resource management strategies, and territorial planning (Posea & Badea, 1984; Rusu, 2007). The shape of the Nera basin and the varied relief, with significant altitude differences, favor the rapid water concentration downstream, increasing the risk of floods, torrential erosion, and landslides, especially in areas with steep slopes and impermeable soils..

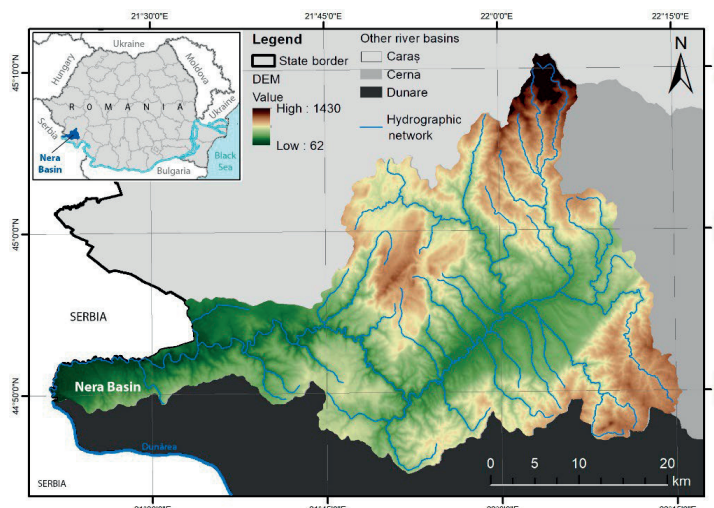


Figure 1. Study area location and Digital Elevation Model (DEM) (processing after EEA-DEM, 2016; Geospatial, 2021)

### The working methodology

The methodology for assessing flood susceptibility in the Nera basin was adapted from the MCDA and AHP models applied through GIS, following the research conducted by Hammami et al. (2019), Swain et al. (2020), GIS and RS Solution and Copăcean et al. (2024). The analysis considered nine main factors in triggering and developing floods:

- **Elevation Factor** highlights the terrain relief and indicates the altitude and position of the land relative to the water level (Kumar et al., 2023). The Elevation factor map was derived from a Digital Elevation Model (DEM) with a spatial resolution of 25 m (EEA, 2016);

- **Distance from River Factor** shows that flood risk is high near rivers and decreases as their distance increases (Vegad et al., 2018). The river distance map was generated in ArcGIS using the Euclidean Distance tool applied to the vector hydrographic network (Geospatial, 2021);

- **Topographic Wetness Index (TWI) Factor** estimates soil moisture levels and areas of water accumulation (Kumar et al., 2023). TWI parameters were derived from DEM, and the TWI map was obtained by applying the relation  $TWI = \ln(\alpha/\tan\beta)$  (Swain et al., 2020), where  $\alpha$  represents the cumulative drainage area per unit contour length, and  $\tan\beta$  is the slope at the contact point;

- **Precipitation Factor**, essential in flood formation (Osman & Das, 2023), influences the susceptibility of the territory by increasing water input and potential runoff (Eriyagama et al., 2017; Kumar et al., 2023). The precipitation factor map was generated based on the amount of rainfall (mm) recorded at meteorological stations near the study area in 2022, a year that experienced significantly higher precipitation than the regional average (Climatic Databases, 2024). Data was integrated into GIS and geostatistically interpolated using the IDW (Inverse Distance Weighting) method;

- **Slope Factor** influences water runoff; on steep slopes, water drains quickly, reducing accumulation, whereas on flat or low-slope terrain, runoff is slower, favoring accumulation (Tehrany & Kumar, 2018). The slope map was generated from DEM and expressed in degrees;

- **Drainage Density Factor** indicates the development of the hydrographic network and is calculated as the ratio between its length and the drained area (Dube, 2018). Higher density implies a higher flood risk (Mitra & Das, 2022). In this study, the drainage density map (km/km<sup>2</sup>) was created using the Line Density tool in ArcGIS, based on the vector hydrographic network;

- **Soil Type Factor** influences water runoff and infiltration through its structure and texture. Clayey soils retain water on the surface, promoting accumulation, while sandy soils allow its infiltration (Anni et al., 2020). The map for this factor was created based on vector soil types (Geospatial, 2021), classified according to flood susceptibility and converted into raster format for analysis;

- **Land Use/Land Cover (LULC) Factor** affects water infiltration, runoff, and flood dynamics (Osman & Das, 2023). In the study area, the LULC map is based on Corine Land Cover 2018 (CLC, 2025) data, classified according to flood susceptibility. Forest areas have the lowest risk, while arable land has the highest. After reclassifying the vector data, the map was rasterized for cumulative analysis;

- **Distance from Road Factor** influences infiltration, as land near roads has reduced permeability, favoring water accumulation (Osman & Das, 2023). For the study area, the road distance map (m) was generated in ArcGIS

using the Euclidean Distance tool applied to the vector road network (Geospatial, 2021).

The nine factors analyzed for assessing the flood susceptibility of the Nera basin were represented as raster maps with a resolution of 25 m, in the WGS 1984 system. Based on the specific values of the study area, they were reclassified into five susceptibility classes (Swain et al., 2020): very low, low, moderate, high, and very high.

To determine the value classes, the Natural Break method in ArcGIS was used, and the weight of each factor was determined using the AHP method (GIS and RS Solution, 2025). The final flood susceptibility map was obtained using the Weighted Overlay tool in ArcGIS, following specific workflow algorithms (ArcGIS Desktop Documentation, 2022). In the final analysis, the factors were weighted as follows: Elevation (m): 14%; Distance from River (m): 14%; TWI (dimensionless): 14%; Precipitation (mm/year): 13%; Slope (degrees): 12%; Drainage density (km/km<sup>2</sup>): 11%; Soil type: 8%; LULC: 8% and Distance from Road (m): 6%.

## RESULTS AND DISCUSSIONS

A comprehensive assessment of flood susceptibility in the Nera Basin was conducted by analyzing nine key factors that influence hydrological risk. By examining these factors, it is possible to identify vulnerable areas and understand the mechanisms that determine the extent and intensity of floods.

The **altitude factor** influences the position of the terrain relative to the water level (Kumar et al., 2023), determining the direction of runoff and water accumulation, with low-lying areas, such as plains, being the most vulnerable to flooding (Hammami et al., 2019).

In terms of altitude, low-lying areas (61 - 335 m) along rivers in the Nera Basin (Figure 2) are the most susceptible to flooding, presenting the highest risk. Intermediate altitudes (336 - 550 m) remain vulnerable but with a lower risk, while transition zones (551-781 m) exhibit moderate susceptibility. In contrast, high-altitude regions (782-1430 m) have minimal risk due to rapid water runoff. An inverse relationship is observed between altitude and flood susceptibility, with low-lying terrains being the most exposed.

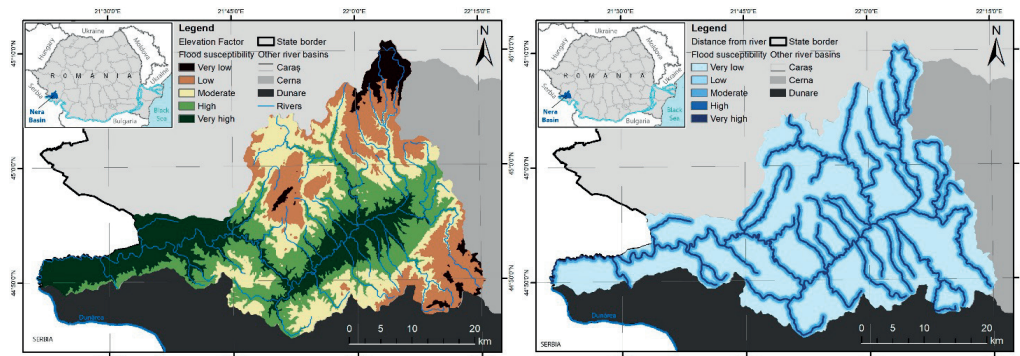


Figure 2. Susceptibility to flooding in the Nera basin based on the Elevation factor - m (left) and the Distance from rivers factor - m (right)

**The distance from rivers factor** (Figure 2) highlights a direct correlation between proximity to watercourses and flood risk (Vegad et al., 2018). Areas located within 0 - 100 m of rivers exhibit very high susceptibility, frequently experiencing flooding during rainy periods. Regions situated 101 - 150 m away have a high risk, those between 151 - 500 m face a moderate risk, while areas at 501 - 700 m show low susceptibility. Zones beyond 701 m are the least exposed to flooding.

**The TWI (Topographic Wetness Index) factor** reflects the terrain's tendency to

accumulate and retain water (Kumar et al., 2023). In the analyzed area, areas with very high susceptibility (TWI 14.68-28.09) are found in valleys and depressions, where water naturally accumulates, presenting the highest flood risk. High susceptibility (TWI 10.21- 14.67) characterizes low-lying areas near rivers. Moderate susceptibility regions (TWI 7.32-10.20) are located in transitional zones, with partial water accumulation. Low and very low susceptibility (TWI 2.64-7.31) is specific to slopes and higher areas, where natural drainage reduces the flood risk (Figure 3).

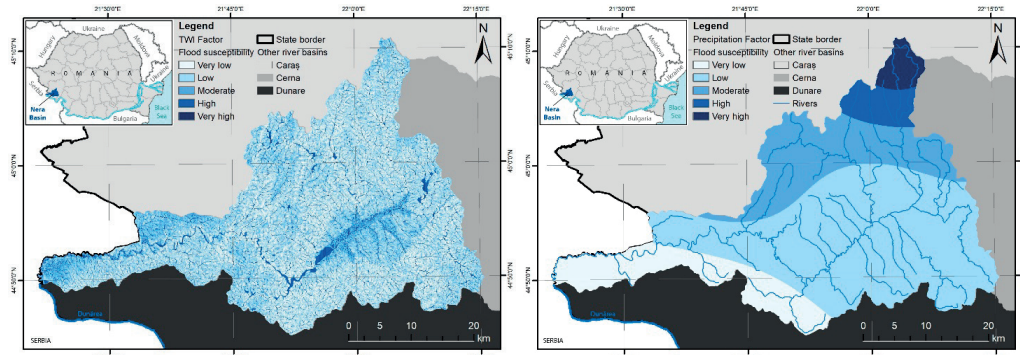


Figure 3. Susceptibility to flooding in the Nera basin based on the TWI factor (left) and the Precipitation factor - mm/year (right)

**The precipitation factor** plays a crucial role in triggering floods, influencing the land's susceptibility through increased water input and intensified surface runoff (Osman & Das, 2023). In the Nera basin, the distribution of flood risk varies depending on the amount of precipitation (Figure 3). Areas with very high susceptibility

(1876-2261 mm) are located in the north, where precipitation is most abundant, significantly increasing flood risk, especially during rainy periods. High susceptibility regions (1562-1875 mm) extend toward the center, indicating a considerable risk. Moderate susceptibility areas (1353-1561 mm) are centrally located, where

precipitation levels are lower, reducing the probability of flooding. In the southern part of the basin, where precipitation is lower, areas with low susceptibility (1221-1352 mm) and very low susceptibility (1098-1220 mm) can be found.

The relationship between **terrain slope** and flood risk is inverse: areas with gentle slopes facilitate water accumulation and present a higher flood risk, whereas regions with steep slopes allow rapid water drainage, reducing vulnerability (Tehrany & Kumar, 2018).

In the Nera basin (Figure 4), areas with very high susceptibility ( $0-6.50^\circ$ ) are found in river floodplains and depressions, where water drains slowly and can stagnate, favoring floods. High susceptibility ( $6.51-12.76^\circ$ ) characterizes transitional areas, where the risk remains significant. Moderate susceptibility ( $12.77-19.26^\circ$ ) is typical for steeper terrains, where water runoff is more efficient. Areas with low and very low susceptibility ( $19.27-64.05^\circ$ ) are located in hilly and mountainous regions, where water is rapidly evacuated, reducing the flood risk.

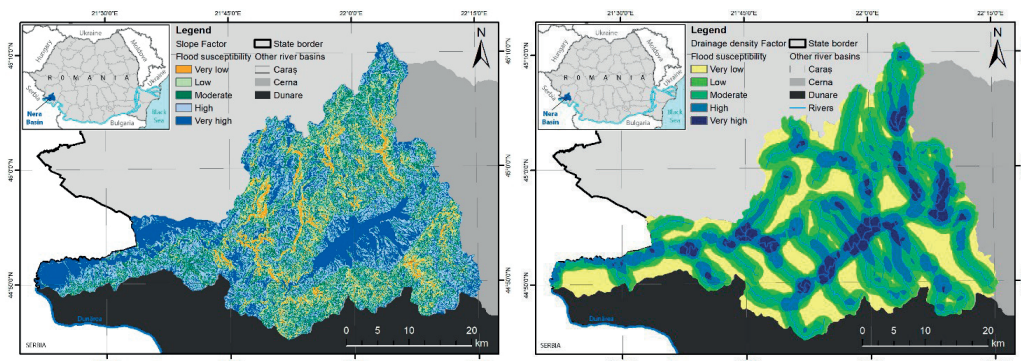


Figure 4. Susceptibility to flooding in the Nera basin based on the Slope factor - degrees (left) and the Drainage density factor -  $\text{km}/\text{km}^2$  (right)

The **drainage density** reflects the degree of fragmentation of the hydrographic network and influences the land's capacity to evacuate water (Mitra & Das, 2022). Areas with high drainage density are more exposed to flooding as they collect and transport a large volume of water. Areas with very high susceptibility ( $0.78-1.22 \text{ km}/\text{km}^2$ ) are located near major rivers and dense secondary watercourses, where water accumulation is frequent. High susceptibility ( $0.54-0.77 \text{ km}/\text{km}^2$ ) extends along watercourses, indicating a significant but lower flood risk. Regions with moderate susceptibility ( $0.35-0.53 \text{ km}/\text{km}^2$ ) are farther from rivers, with a lower risk of water accumulation.

Areas with low susceptibility ( $0.15-0.34 \text{ km}/\text{km}^2$ ) and very low susceptibility ( $0-0.14 \text{ km}/\text{km}^2$ ) are situated in regions with poorly developed drainage, where the probability of flooding is minimal (Figure 4).

The **type of soil** influences the degree of water infiltration and runoff, determining the flood risk level (Anni et al., 2020). Areas with very high susceptibility correspond to clay soils (Figure 5). These have very low permeability, favoring water accumulation and increasing the flood risk. Such soils are predominant in lowland areas and near rivers.

Regions with moderate susceptibility are associated with medium-textured soils. These allow partial water infiltration, reducing the flood risk compared to clay soils but still having limited drainage capacity. Areas with low susceptibility consist of sandy soils, which have high permeability, allowing rapid water infiltration and thus reducing the flood risk. These regions are less exposed to surface water accumulation.

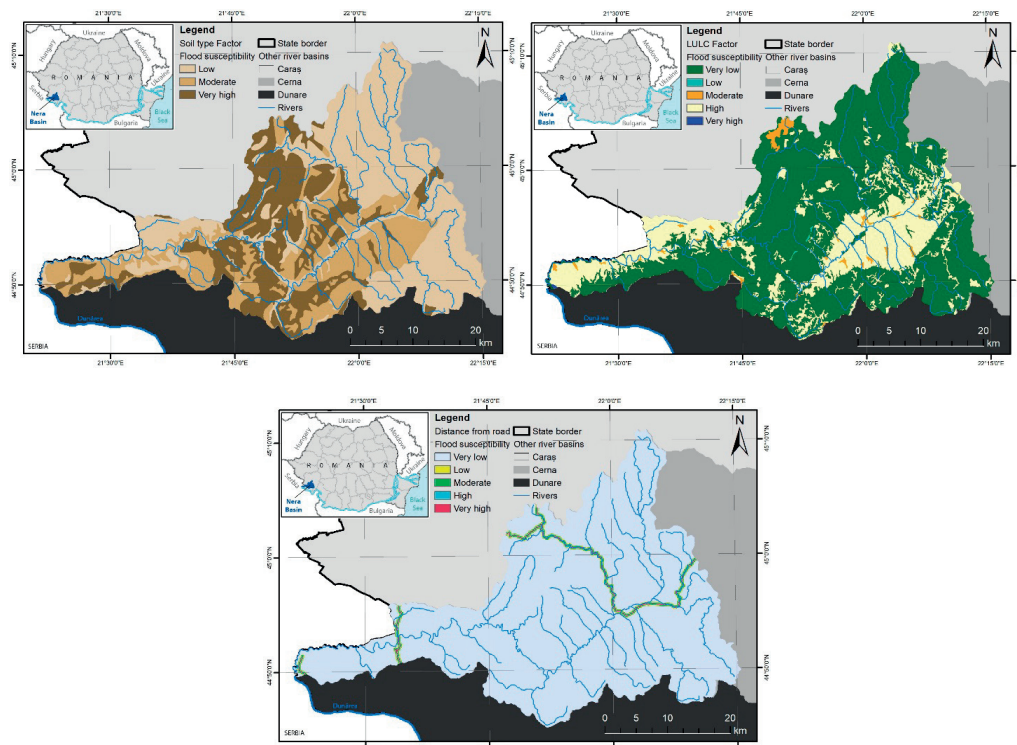


Figure 5. Susceptibility to flooding in the Nera basin based on the Soil Types factor (left), the Land Use/Land Cover factor (right), and the Distance to Roads factor - m (center)

**LULC** influence the water infiltration capacity, determining the degree of flood vulnerability (Osman & Das, 2023). Areas with very high susceptibility are those covered by water, where accumulation is permanent, presenting the highest flood risk (Figure 5). Agricultural lands, with low permeability, have high susceptibility, being exposed to flooding during periods of heavy rainfall. Built-up areas exhibit moderate susceptibility, as they reduce water infiltration and promote accumulation in the absence of adequate drainage. In contrast, areas covered by dense vegetation, especially forests, have very low susceptibility.

**The Distance from Road (m)** factor influences the water infiltration and accumulation capacity (Osman & Das, 2023). Areas with very high susceptibility (0-50 m) are located to the near roads (Figure 5). In these areas, the flood risk is at its maximum due to insufficient drainage or obstruction of natural runoff. Regions with high susceptibility (51-100 m) are also near roads, where the effect of water accumulation is significant but slightly less intense. Areas with

moderate susceptibility (101-200 m) are situated at greater distances from roads and have a lower flood risk. Regions with low susceptibility (201-300 m) and very low susceptibility (>301 m) are located far from roads, where the terrain allows for better water infiltration and dispersion, reducing flood risk.

Based on the nine factors analyzed previously, a flood susceptibility map was generated, and by applying the Weighted Overlay Analysis (WOA) method, the final distribution of areas with different degrees of vulnerability was obtained (Figure 6).

The area with very low susceptibility represents only 441 ha, equivalent to 0.32% of the basin, indicating a minimal flood risk in these territories. The low susceptibility zone occupies the largest area of the basin, covering 72,356 ha, representing 52.4% of the total. This zone is predominantly located in regions less exposed to water accumulation. The moderate susceptibility zone covers 59,498 ha, or 43.1% of the basin. These regions lie in the transition between lowland and highland areas, presenting

a considerable flood risk. The high susceptibility zone extends over 5,784 ha (4.2%), being

concentrated near watercourses, where water accumulation is frequent.

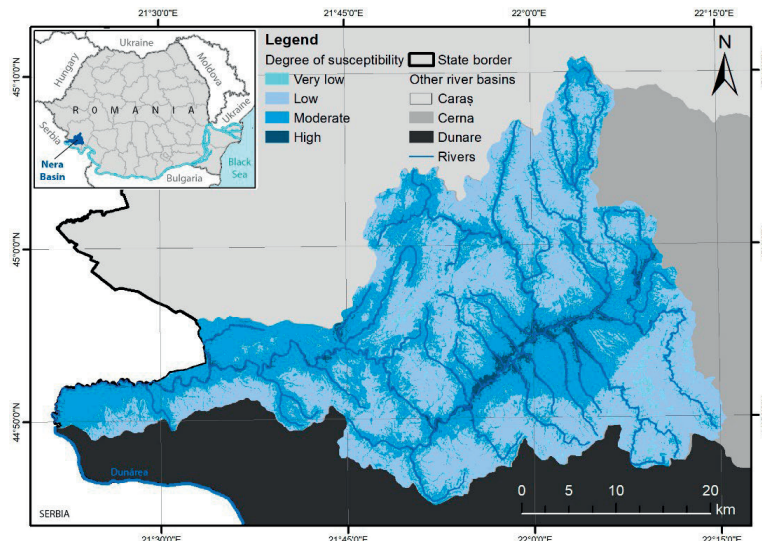


Figure 6. Flood susceptibility map in the Nera basin

The map in Figure 6 indicates a prevalence of low and moderate susceptibility classes, suggesting that most of the basin is not highly exposed to flooding. However, areas located near rivers require special preventive measures. The flood susceptibility analysis in the Nera basin provides a clear picture of the distribution of areas at hydrological risk (Figure 6). However, for a more detailed assessment of the effects of these phenomena, it is essential to examine and analyze the impact of floods, with varying intensities, on different types of LULC. Floods affect soil properties, agricultural fertility, and ecosystem functioning, with a significant impact on land use (Furtak & Wolińska, 2023; Rupngam & Messiga, 2024).

In the analyzed area, forests represent the most extensive type of land cover (Table 1), occupying 97,322 ha. Among these, 30,233 ha (31%) are exposed to moderate risk, while only 794 ha (0.8%) fall into the high-risk category, confirming the role of forests in reducing the impact of floods. Artificial areas (settlements, infrastructure) total 2,213 ha, with 1,954 ha (88.3%) classified under moderate and high susceptibility categories, indicating a significant vulnerability of urban infrastructure to flooding. Bare soils cover a very small area (86 ha) and are mainly affected by low or moderate susceptibility floods.

Table 1 The impact of floods on different types of LULC in the Nera River basin

LULC classes	Flood susceptibility degree (ha)				
	Very low	Low	Moderate	High	Total (ha)
Artificial surfaces	0	293	1543	411	2213
Forest areas	467	65828	30233	794	97322
Agricultural land	1	6087	27704	4635	38426
Bare soil	1	82	2	0	86
Total (ha)	469	72290	59485	5840	138084

Agricultural lands cover a total of 38,426 hectares, of which 32,339 hectares (84.2%) are classified as moderate or high susceptibility to

flooding. Only 6,087 hectares (15.8%) are located in a low-risk area, indicating a limited percentage of agricultural land protected from

floods. Following flood events, arable lands are the most vulnerable, as nutrient losses and the accumulation of toxic metabolites reduce crop yields (Rupngam & Messiga, 2024). In the case of grasslands, flooding induces physiological stress on plants, which can lead to biodiversity loss (Călușeru et al., 2013; Pedersen & Colmer, 2013). Additionally, soils may undergo structural changes, reducing drainage capacity and long-term fertility, which impacts vegetation regeneration and the use of land for agricultural or pastoral activities (Copăcean et al., 2020; Barneze et al., 2023).

## CONCLUSIONS

The analysis of factors influencing flood susceptibility in the Nera basin has highlighted that elevation, distance from rivers, Topographic Wetness Index (TWI), precipitation, slope, drainage density, soil type, land use/land cover, and distance from roads play a crucial role in determining vulnerable areas. Factors related to terrain positioning and hydrological characteristics directly influence water accumulation and drainage. Low-lying areas close to watercourses with poorly permeable soils are the most exposed to flood risks.

The flood susceptibility map of the Nera basin, classified based on susceptibility levels, shows that most of the analyzed area falls into low and moderate susceptibility categories, covering over 95% of the total surface. However, approximately 4% of the territory is at high risk, concentrated in lowland areas along rivers where water accumulation is frequent. This underscores the importance of implementing prevention and risk management measures, particularly in regions vulnerable to flooding.

The impact of floods on LULC classes is significant, with agricultural lands being the most affected. Over 84% of these areas are in moderate and high susceptibility zones, making them vulnerable to nutrient loss, decreased productivity, and soil degradation.

Geomatic models, through the integration and analysis of spatial data, have proven to be essential tools in flood susceptibility assessment. These models enable detailed risk mapping and the identification of vulnerable areas, providing scientific support for decision-

making regarding territorial planning and prevention measures. The application of GIS techniques and the Weighted Overlay Analysis method demonstrates the importance of multidisciplinary approaches in managing natural hazards, contributing to the development of effective strategies for reducing flood impact.

## REFERENCES

Anni, A.H., Cohen, S., & Praskiewicz, S. (2020). Sensitivity of urban flood simulations to stormwater infrastructure and soil in-filtration. *J Hydrol*, 588, <https://doi.org/10.1016/j.jhydrol.2020.125028>

Arabameri, A., Saha, S., Chen, W., Roy, J., Pradhan, B., & Bui, D.T. (2020). Flash flood susceptibility modelling using functional tree and hybrid ensemble techniques. *J. Hydrol.*, 587, 125007. <https://doi.org/10.1016/j.jhydrol.2020.125007>

ArcGIS Desktop Documentation. (2022). ArcMap (Including ArcCatalog, ArcScene, ArcGlobe), <https://desktop.arcgis.com/en/documentation/> (accessed on 15 June 2022)

Barneze, A.S., van Groenigen, J.W., Philippot, L., Bru, D., Abalos, D., & De Deyn, G.B. (2023). Plant communities can attenuate flooding induced N2O fluxes by altering nitrogen cycling microbial communities and plant nitrogen uptake. *Soil Biol. Biochem.*, 185, 109142. <https://doi.org/10.1016/j.soilbio.2023.109142>

Bharadwaj, B., Mishegyan, A., Nagalingam, S., Guenther, A., Joshee, N., Sherman, S.H., & Basu, C. (2023). Physiological and genetic responses of lentil (*Lens culinaris*) under flood stress. *Plant Stress*, 7, 100130. <https://doi.org/10.1016/j.stress.2023.100130>

Cai, S., Fan, J., & Yang, W. (2021). Flooding Risk Assessment and Analysis Based on GIS and the TFN-AHP Method: A Case Study of Chongqing, China. *Atmosphere*, 12(5), 623. <https://doi.org/10.3390/atmos12050623>

Călușeru, A.L., Cojocariu, L., Horablagă, M.N., Bordean, D.-M., Horablagă, A., Cojocariu, A., Borozan A.B., & Iancu, T. (2013). Romanian National Strategy for the conservation of biodiversity 2013 – 2020 – integration of european environmental policies. *SGEM Conf Proceedings*, 2, 723-728. <https://doi.org/10.5593/SGEM2013/BE5.V2/S23.013>

Chen, J., Zhang, Y., Chen, Z., & Nie, Z. (2015). Improving assessment of groundwater sustainability with analytic hierarchy process and information entropy method: A case study of the Hohhot Plain, China. *Environ. Earth Sci.*, 73, 2353–2363. <https://doi.org/10.1007/s12665-014-3583-0>

Climatic Database. (2024). [https://rp5.ru/Weather\\_in\\_Romania](https://rp5.ru/Weather_in_Romania) (accessed on 15.11.2024)

Copăcean, L., Cojocariu, L., Simon, M., Zisu, I., & Popescu, C. (2020). Geomatic techniques applied for remote determination of the hay quantity in agrosilvopastoral systems. *Present Environ. Sustain.*

Dev., 14, 89–101.  
<https://doi.org/10.15551/pesd2020142006>

Copăcean, L., Man, E.T., Herban, S., Popescu, C.A., & Cojocariu, L. (2024). Estimating flood susceptibility based on GIS and remote sensing. Case study: Hydrographic Basin of Crisul Alb river. *Present Environ. Sustain. Dev.*, 18(1), 121-140. <https://doi.org/10.47743/pesd2024181009>

Copăcean, L., Man, E.T., Cojocariu, L.L., Popescu, C.A., Vilceanu, C.-B., Beilicci, R., Crețan, A., Herbei, M.V., Cuzic, O.Ş., & Herban, S. (2025). GIS-Based Flood Assessment Using Hydraulic Modeling and Open Source Data: An Example of Application. *Appl. Sci.*, 15, 2520. <https://doi.org/10.3390/app15052520>

Corine Land Cover - CLC (2025). Copernicus Land Monitoring Service. Available online: <https://land.copernicus.eu/pan-european/corine-land-cover> (accessed on 10.02.2025)

Costache, R., & Zaharia, L. (2017). Flash-flood potential assessment and mapping by integrating the weights-of-evidence and frequency ratio statistical methods in GIS environment - Case study: Bâscă Chiojdului River catchment (Romania). *J Earth Syst Sci*, 126, 59. <https://doi.org/10.1007/s12040-017-0828-9>

Covaci, O., Gazda, M.R., Niga, B.I., Enea, A., Iosub, M., & Tîrnovan, A. (2023). Automation of the Rational Formula using GIS infrastructure - Case study Siret River Basin - Romania. *Present Environ. Sustain. Dev.*, 17(2), 31–44. <https://doi.org/10.47743/pesd2023172003>

Dragomir, A., Tudorache, A.-V., & Costache, R.-D. (2020). Assessment of flash-flood susceptibility in small river basins. *Present Environ. Sustain. Dev*, 14(1), 119-130. <https://doi.org/10.15551/pesd2020141010>

Dube, M. (2018). Bihar Floods: A Report on Bihar Floods 2016; Bihar Disaster Management Authority, Government of Bihar: Patna, India; p. 36

Eriyagama, N., Thilakarathne, M., Tharuka, P., Munaweera, T., Muthuwatta, L., Smakhtin, V., Premachandra, W.W., Pindeniya, D., Wijayarathne, N.S., & Udamulla, L. (2017). Actual and perceived causes of flood risk: Climate versus anthropogenic effects in a wet zone catchment in Sri Lanka. *Water Int*, 42, 874–892, <https://doi.org/10.1080/02508060.2017.1373321>

European Environment Agency (EEA). (2016). Digital Elevation Model (DEM), <https://www.eea.europa.eu/data-and-maps/data/copernicus-land-monitoring-service-eu-dem> (accessed on 13.12.2016)

Furtak, K., & Wolińska, A. (2023). The impact of extreme weather events as a consequence of climate change on the soil moisture and on the quality of the soil environment and agriculture - A review. *Catena*, 231, 107378. <https://doi.org/10.1016/j.catena.2023.107378>

Geospatial. (2021). România: seturi de date vectoriale generale – <http://geospatial.org/vechi/download/romania-seturi-vectoriale> (accessed on 10.01.2021)

GIS & RS Solution. (2025). Flood Susceptibility Mapping using GIS-AHP Multi-criteria Analysis. Available online: <https://www.youtube.com/watch?v=Lbbyi1YV2Hc&list=RDCMUCs1fLqqz84QbQ89DnRmMEVQ&index=1> (accessed on 10.02.2025)

Hagos, Y.G., Andualem, T.G., & Yibeltal, M. et al. (2022). Flood hazard assessment and mapping using GIS integrated with multi-criteria decision analysis in upper Awash River basin, Ethiopia. *Appl Water Sci*, 12, 148. <https://doi.org/10.1007/s13201-022-01674-8>

Hammami, S., Zouhri, L., & Souissi, D. et al. (2019). Application of the GIS based multi-criteria decision analysis and analytical hierarchy process (AHP) in the flood susceptibility mapping (Tunisia). *Arab J Geosci*, 12, 653. <https://doi.org/10.1007/s12517-019-4754-9>

Khosh Bin Ghomash, S., Bachmann, D., Caviedes-Voullième, D., & Hinz, C. (2022). Impact of Rainfall Movement on Flash Flood Response: A Synthetic Study of a Semi-Arid Mountainous Catchment. *Water*, 14, 1844. <https://doi.org/10.3390/w14121844>

Kumar, R., Kumar, M., Tiwari, A., Majid, S.I., Bhadwal, S., Sahu, N., & Avtar, R. (2023). Assessment and Mapping of Riverine Flood Susceptibility (RFS) in India through Coupled Multicriteria Decision Making Models and Geospatial Techniques. *Water*, 15, 3918. <https://doi.org/10.3390/w15223918>

Mitra, R., & Das, J. (2022). A comparative assessment of flood susceptibility modelling of GIS-based TOPSIS, VIKOR, and EDAS techniques in the sub-himalayan foothills region of Eastern India. *Environ Sci Pollut Res*, 30, 16036–16067. <https://doi.org/10.1007/s11356-022-23168-5>

Osman, S.A., & Das, J. (2023). GIS-based flood risk assessment using multi-criteria decision analysis of Shebelle River Basin in southern Somalia. *SN Appl Sci*, 5, 134. <https://doi.org/10.1007/s42452-023-05360-5>

Papaioannou, G., Efstratiadis, A., Vasilades, L., Loukas, A., Papalexiou, S.M., Koukovinos, A., Tsoukalas, I., & Kossieris, P. (2018). An operational method for flood directive implementation in ungauged urban areas. *Hydrology*, 5, 24. <https://doi.org/10.3390/hydrology5020024>

Pedersen, O., & Colmer, T.D., (2013). Sand-Jensen, K. Underwater photosynthesis of submerged plants - recent advances and methods. *Front. Plant Sci.*, 4, 140. <https://doi.org/10.3389/fpls.2013.00140>

Peker, İ.B., Gülbaz, S., Demir, V., Orhan, O., & Beden, N. (2024). Integration of HEC-RAS and HEC-HMS with GIS in Flood Modeling and Flood Hazard Mapping. *Sustainability*, 16, 1226. <https://doi.org/10.3390/su16031226>

Popescu, N.C., & Bărbulescu, A. (2023). Flood Hazard Evaluation Using a Flood Potential Index. *Water*, 15, 3533. <https://doi.org/10.3390/w15203533>

Posea, G., & Badea, L. (1984). România. *Unităile de relief (Regionarea geomorfologică)*, Ed. Științifică și Enciclopedică, București

Rupngam, T., & Messiga, A.J. (2024). Unraveling the Interactions between Flooding Dynamics and Agricultural Productivity in a Changing Climate. *Sustainability*, 16, 6141. <https://doi.org/10.3390/su16146141>

Rusu, R. (2007). *Organizarea spațiului geografic în Banat*, Ed. Mirton, Timișoara.

Simon, M., Copăcean, L., & Cojocariu, L. (2022). Techniques for identification, mapping and analysis of grasslands. Case study: Arad county. *PESD*, 16(2), 39–49. <https://doi.org/10.47743/pesd2022162004>

Souissi, D., Zouhri, L., Hammami, S., Msaddek, M.H., Zghibi, A., & Dlala, M. (2019). GIS-based MCDM-AHP modeling for flood susceptibility mapping of arid areas, southeastern Tunisia. *Geocarto Int*, 35, 991–1017. <https://doi.org/10.1080/10106049.2019.1566405>

Swain, K.C., Singha, C., & Nayak, L. (2020). Flood Susceptibility Mapping through the GIS-AHP Technique Using the Cloud. *ISPRS Int J Geo-Inf*, 9, 720. <https://doi.org/10.3390/ijgi9120720>

Syarifudin, A., Satyanaga, A., & Destania, H.R. (2022). Application of the HEC-RAS Program in the Simulation of the Streamflow Hydrograph for Air Lakitan Watershed. *Water*, 14, 4094. <https://doi.org/10.3390/w14244094>

Tehrany, M.S., & Kumar, L. (2018). The application of a Dempster-Shafer-based evidential belief function in flood susceptibility mapping and comparison with frequency ratio and logistic regression methods. *Environ Earth Sci*, 77, 490. <https://doi.org/10.1007/s12665-018-7667-0>

Vegad, U., Pokhrel, Y., Mishra, V., Ghosh, A., & Kar, S.K. (2018). Application of analytical hierarchy process (AHP) for flood risk assessment: A case study in Malda district of West Bengal, India. *Hydrol. Earth Syst Sci Discuss*, 94, 349–368. <https://doi.org/10.1007/s11069-018-3392-y>

Wang, X., Liu, Z., & Chen, H. (2022). Investigating Flood Impact on Crop Production under a Comprehensive and Spatially Explicit Risk Evaluation Framework. *Agriculture*, 12, 484. <https://doi.org/10.3390/agriculture12040484>